UNIVERSITY OF CHEMICAL TECHNOLOGY AND METALLURGY
Faculty of Chemical and Systematic Engineering
Department of Chemical Engineering

UTILIZATION OF AGRO-LIGNOCELLULOSIC MATERIALS FOR THE REMOVAL OF BASIC DYES FROM AQUEOUS SOLUTIONS

By

Taha Farghaly Hassanein

SUMMARY

For Dissertation Submitted In Partial Fulfillment
of the Requirements for the Degree of

Doctor of Philosophy

Under Supervision of

Prof. Dr. Eng. Bogdana Koumanova

Sofia, Bulgaria

2011

The Ph.D. thesis is written on 118 pages and contains 48 figures and 14 tables. 244 literature sources are cited.

The presented thesis has been considered and accepted for a defense on a meeting of the scientific council of the Department of Chemical Engineering on 3rd December, 2010.

The public defense of the Ph.D. thesis will be held on 02.06.2011 at 14.30 h in hall 424, bld. A of UCTM.
The materials are available on Internet web site of UCTM and in the office “Research Activities”, room 406, 4th floor, bld. A of UCTM.

CONTENTS

Introduction

From an environmental point of view, the removal of synthetic dyes is of great concern, since some dyes and their degradation products may be carcinogens and toxic. The adsorption technique is proved to be an effective and attractive process for the treatment of these dye-bearing wastewaters.

In wastewater treatment the activated carbon is the most popular adsorbent but certain problems with the high cost and regeneration limit its application. At present, there is a growing interest in using other low-cost adsorbents.

There has been much interest in the use of agricultural wastes as adsorbents to prevent and remediate environmental contamination by dyes. Undoubtedly, agricultural wastes offer a lot of promising advantages for use as adsorbents. Agricultural wastes are low-cost, abundantly available and mainly composed of cellulose, hemicelluloses and lignin which make them effective adsorbents for a wide range of pollutants due to the presence of functional groups such as hydroxyl, carboxyl, methoxy, phenols, etc., that participate in the binding to pollutants.

1. Conclusions from literature review

A literature review was presented which is concerned with dyes wastes, different technologies for their removal focusing on adsorption as a superior and effective method for dyes removal. This review presented the different adsorbents used for the treatment of dyes from aqueous solutions.

The review presented low-cost adsorbents utilized for the removal of dyes such as natural materials (clays, zeolites, and silicates), biosorbents (chitin and chitosan, peat, and biomass) and waste materials from industry (fly ash, red mud and sludge) and agriculture.

This review was focused on using agricultural wastes as-received (unmodified), after converted into activated carbons or after being modified for the removal of dyes from their aqueous solutions with investigating adsorption equilibrium isotherms and kinetic studies.

As most industrial wastewaters contain more than one dye (as a mixture), the review was also presented some adsorbents used for the removal of dyes from binary- and multi-component systems. The results presented in this review indicated that agricultural wastes are promising adsorbents for environmental and purification purposes.

2. Aim and tasks of dissertation

The aim of this dissertation is study on the feasibility of using the agricultural wastes, *flax shives* (FS) and *wheat straw* (WS) as low-cost adsorbents for decolourisation of wastewaters as alternatives to expensive commercial adsorbents.

The following tasks were carried out in the course of this work:

1. Investigating the adsorption potential of FS and WS for the removal of Basic Yellow 21 (BY 21) from single solution system.

2. Equilibrium modeling studies using model aqueous solutions of Basic Yellow 21 for adsorption on both FS and WS by the application of equilibrium isotherm models such as Langmuir, Freundlich and Temkin to find the most suitable model that can be used for design purpose.

3. Studying the individual and simultaneous removal of Basic Blue 3 (BB 3) and Basic Red 18 (BR 18) dyes from aqueous solutions using FS and WS and comparing with single dye system in a batch mode.

4. Determination of the applicability of non-competitive single-component Langmuir and Freundlich adsorption isotherm models for adsorption of BB 3 and BR 18 onto FS and WS from single- and binary-component systems and also examination of the applicability of the multi-component modified Langmuir and Sheindorf–Rebuhn–Sheintuch (SRS) adsorption isotherm models to the competitive adsorption equilibrium of the dyes in binary systems.

5. Studying the effect of operating parameters such as dye concentration, adsorbent dosage and stirring rate on the kinetics of Basic Yellow 21 adsorption onto FS and WS.

6. Interpretation of the adsorption mechanism, through the application of kinetic models such as pseudo-first order, pseudo-second order and intraparticle diffusion models that describe the kinetic data for the adsorption of BY 21, BB 3 and BR 18 on FS and WS in single- or binary-component systems.

3. Materials, methods, and results

3.1. Materials and methods

3.1.1. Adsorbates

The dyes used as adsorbates in the present study were Basic Yellow 21 (BY 21), Basic Blue 3 (BB 3) and Basic Red 18 (BR 18), whose chemical structures and general characteristics are depicted in Fig. 1.

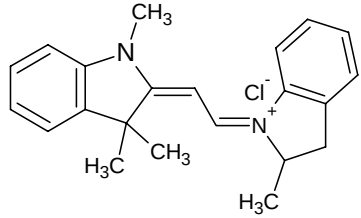

(a) **Basic Yellow 21**

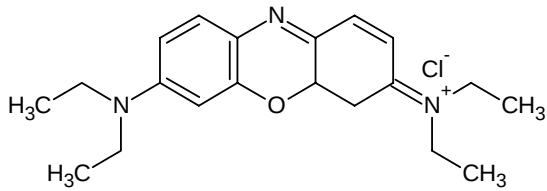

(b) **Basic Blue 3**

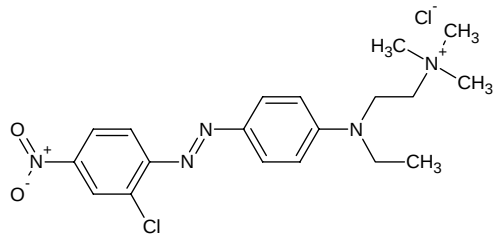

(c) **Basic Red 18**

Fig. 1. Chemical structures of (a) Basic Yellow 21, (b) Basic Blue 3 and (c) Basic Red 18.

3.1.2. Adsorbents

Two Egyptian agricultural wastes were used as adsorbents, flax shives (FS) and wheat straw (WS). Prior to use in the experiments, FS were crushed to fine particles of about 0.2 mm size. WS was collected from Egyptian fields and used as received without any pretreatment.

3.1.3. Chemical characterization of adsorbents

The chemical compositions of FS and WS were described in Table 1 which indicates that FS and WS are composed mainly of cellulose, hemicellulose and lignin, which provides binding sites for the dyes due to the presence of functional groups such as hydroxyl, carboxyl, methoxy, phenols, etc.

Table 1. Chemical composition (%) of FS and WS.

Adsorbent	α-Cellulose	Hemicellulose	Lignin	Extractives	Ash
FS	56.2	16	23	3.2	1.6
WS	41.5	32.1	17	5.8	3.6

3.1.4. Analysis of dye concentration

3.1.4.1. Analysis in single-component systems

The concentrations of dyes in single-component systems were measured by means of a spectrophotometer (Spekol 11, Carl Zeiss JENA) by monitoring the absorbance changes at wavelengths of maximum absorbance (λ_{max}) of 416, 610 and 488 nm for BY 21, BB 3 and BR 18, respectively, using a standard calibration curves.

3.1.4.2. Analysis in binary-component systems

Suppose that there is no interaction between the two dyes in binary-component systems, the total absorbance for a mixture dye solution is equal to the summation of the absorbance of each dye. This is represented in Eq. (1). To determine and analyse whether the existence of one dye affected the adsorption of another dye, the adsorption capacities of each dye in mixture solutions are computed using Eqs. (2) and (3).

$$A_{\lambda} = A_{BB} + A_{BR} \tag{1}$$

$$A_{\lambda 1} = \varepsilon_{1BB} l C_{BB} + \varepsilon_{1BR} l C_{BR} \tag{2}$$

$$A_{\lambda 2} = \varepsilon_{2BB} l C_{BB} + \varepsilon_{2BR} l C_{BR} \tag{3}$$

where: A_{λ}, $A_{\lambda 1}$ and $A_{\lambda 2}$ are the absorbance of spectrometer at wavelengths λ, λ_1 and λ_2, respectively; A_{BB} and A_{BR} are the absorbance of BB 3 and BR 18 dyes at wavelength λ, respectively; ε_{1BB} and ε_{2BB} are the molar absorptivities of pure BB 3 at wavelengths λ_1 and λ_2, respectively; ε_{1BR} and ε_{2BR} are the molar absorptivities of pure BR 18 at wavelengths λ_1 and λ_2, respectively; C_{BB} and C_{BR} are the concentrations of BB 3 and BR 18 in the mixture solutions; l is the cell width (1 cm); λ_1 (610 nm) is the wavelength of maximum absorbance for BB 3; and λ_2 (488 nm) is the wavelength of maximum absorbance for BR 18.

The concentrations C_{BB} and C_{BR} are solved from Eqs. (2) and (3) and then calculated to obtain the adsorption capacity for each dye in mixture solutions.

3.2. Adsorption Equilibrium

The analysis of the isotherm data by fitting them to different isotherm models is an important step to find the suitable model that can be used for design purpose. The equilibrium modeling of the isotherm studies was divided into two parts: single-component and binary-component equilibrium studies.

3.2.1. Equilibrium modeling for single-component systems

3.2.1.1. Equilibrium isotherm experiment

The adsorption of BY 21 from aqueous solution onto FS and WS was performed using batch equilibrium technique at 20±2 ^{o}C. For the determination of adsorption isotherms, a series of stoppered 100 cm^3 Erlenmeyer flasks were used and each flask was filled with 50 cm^3 of dye solution of varying initial concentration (70 to 550 mg dm^{-3}). A fixed amount of adsorbent (0.5 g) was then added into each flask. The flasks were kept on a platform shaker at a fixed rate for 48 h that was sufficient to establish the equilibrium.

After this period, the mixture was allowed to settle and the supernatant solution was filtered off using syringe filter unit (Minisart®) of 0.2 µm in size and the equilibrium concentrations of dye was measured by the spectrophotometer. The amount of the dye adsorbed at equilibrium (q_e, mg g^{-1}) and the removal percentage (R %) was calculated according to the expressions:

$$q_e = \frac{(C_0 - C_e)V}{m} \tag{4}$$

$$R\,\% = \left[\frac{(C_0 - C_e)}{C_0}\right] 100 \tag{5}$$

where: C_0 and C_e are the initial and equilibrium dye concentrations (mg dm^{-3}), respectively, V is the solution volume (dm^3), and m is the mass of adsorbent (g).

3.2.1.2. Single-component models

In this work, three models were used to describe the relationship between the amount of dye adsorbed, q_e and its equilibrium concentration, C_e. These were Langmuir, Freundlich and Temkin adsorption isotherms.

3.2.1.2.1. Langmuir model

The Langmuir equation and its linear form can be expressed as;

$$q_e = \frac{q_m b C_e}{1 + b C_e} \tag{6}$$

$$\frac{C_e}{q_e} = \frac{1}{q_m b} + \frac{C_e}{q_m} \tag{7}$$

where: q_e is the dye uptake at equilibrium (mg g^{-1}), C_e is the concentration of the solution at equilibrium (mg dm^{-3}), while b (dm^3 g^{-1}) and q_m (mg g^{-1}) are related to the affinity and maximum sorption capacity, respectively.

3.2.1.2.2. Freundlich model

The Freundlich adsorption isotherm equation and its linear form can be expressed as;

$$q_e = K_F C_e^{1/n} \tag{8}$$

$$\log q_e = \log K_F + {}^1/_n \log C_e \tag{9}$$

where: K_F is the Freundlich constant representing the adsorption capacity (dm^3 g^{-1}), and n is the Freundlich exponent that depicting the adsorption intensity.

3.2.1.2.3. Temkin model

The Temkin equation and its linear form can be expressed as;

$$q_e = \frac{RT}{b} \ln(AC_e) \tag{10}$$

$$q_e = B \ln A + B \ln C_e \tag{11}$$

where: A and B are the Temkin isotherm constants. A represents the equilibrium binding constant (dm^3 g^{-1}) and B is the heat of adsorption and $B = RT/b$.

3.2.1.3. Equilibrium modeling for adsorption of Basic Yellow 21 on flax shives

A comparison is made among the three isotherms plotted in Fig. 2, which shows the experimental data points and the three theoretical isotherms (q_e versus C_e) for BY 21 onto FS plotted on the same graph.

The figure clearly indicates that the adsorption capacity, q_e increases initially in a linear way with rising equilibrium concentration, suggesting that the adsorption sites on FS were sufficient. The increase in curvature of the isotherms, as it tends to a monolayer, as C_e values increase considerably for the small increase in q_e, is possibly due to the less active sites being available at the end of the sorption process. Adsorption capacity, q_e is eventually limited by the fixed number of active sites on the FS and a resulting plateau can be observed.

The Langmuir, Freundlich and Temkin isotherm parameters were obtained by plotting C_e/q_e versus C_e (Fig. 3), log q_e versus log C_e (Fig. 4) and q_e versus ln C_e (Fig. 5), respectively. The isotherms constants and the related correlation coefficients were given in Table 2. The best-fit equilibrium model was determined based on the linear regression correlation coefficient R^2. As seen from Table 2, the comparison of R^2 values indicates that the Temkin isotherm best fits the experimental results.

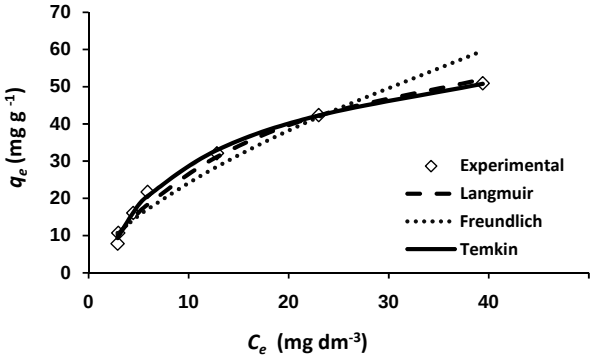

Fig. 2. Adsorption isotherms for BY 21 on FS.

Table 2. Langmuir, Freundlich and Temkin isotherm constants for the adsorption of BY 21 on FS.

Langmuir			**Freundlich**			**Temkin**		
b (dm^3 g^{-1})	q_m (mg g^{-1})	R^2	K_F (dm^3 g^{-1})	n	R^2	B	A (dm^3 g^{-1})	R^2
0.053	76.92	0.946	5.32	1.54	0.929	15.92	0.618	0.996

3.2.1.4. Equilibrium modeling for adsorption of Basic Yellow 21 on wheat straw

Fig. 6 shows the comparative fit of Langmuir, Freundlich and Temkin isotherms with the equilibrium data plotted as q_e versus C_e. From the figure, it can be seen that the equilibrium adsorption capacity, q_e increased with the increase in dye concentration with the observation of a plateau. Linear plots of Langmuir, Freundlich and Temkin isotherms are

obtained. As can be observed in Table 3, the Temkin model provides the best correlation with the equilibrium data.

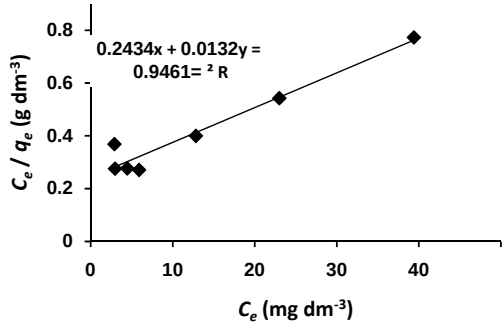

Fig. 3. Langmuir adsorption isotherm for BY 21 on FS.

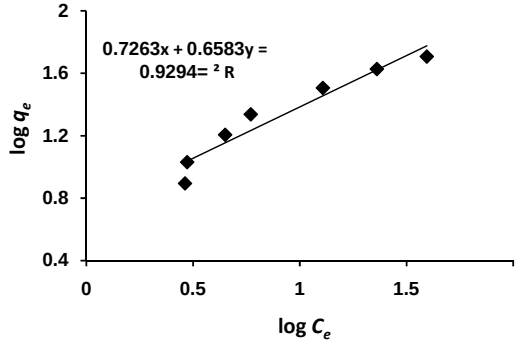

Fig. 4. Freundlich adsorption isotherm for BY 21 on FS.

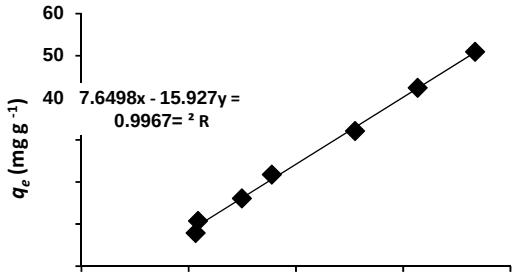

Fig. 5. Temkin adsorption isotherm for BY 21 on FS.

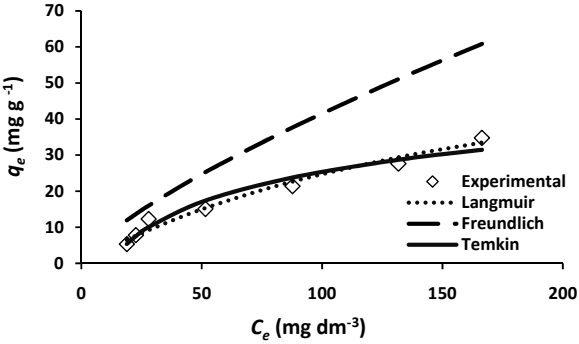

Fig. 6. Adsorption isotherms of BY 21 onto WS.

Table 3. Langmuir, Freundlich and Temkin isotherm constants for the adsorption of BY 21 on WS .

Langmuir			Freundlich			Temkin		
b (dm^3 g^{-1})	q_m (mg g^{-1})	R^2	K_F (dm^3 g^{-1})	n	R^2	B	A (dm^3 g^{-1})	R^2
0.0053	71.43	0.781	0.758	1.33	0.946	12.04	0.082	0.959

3.2.1.5. Comparison between flax shives and wheat straw for adsorption equilibrium of Basic Yellow 21

The values of Langmuir, Freundlich and Temkin isotherms constants for the adsorption of BY 21 on FS and WS are compared in Table 4. It is seen from the table that the maximum adsorption capacity, q_m is in the order FS > WS, which is found to be 76.92 mg g^{-1} and 71.43 mg g^{-1} for FS and WS, respectively. The higher q_m for FS over WS is due to FS has a lower particle size (higher surface area) as compared to WS that has a larger particle size (lower surface area).

3.2.2. Equilibrium modeling for single- and binary-component systems

As most industrial wastewaters contain more than one dye, an investigation on the simultaneous adsorption of Basic Blue 3 (BB 3) and Basic Red 18 (BR 18) onto FS and WS from binary system was studied and compared with single dye system in a batch mode.

3.2.2.1. Equilibrium isotherm experiment

Sorption studies were conducted in a routine manner by the batch technique. A number of stoppered 100 cm^3 Erlenmeyers flasks containing a definite volume (50 cm^3 in each case)

of solutions at desired level of each component were placed in a shaker at 20 °C. For isotherm studies, 0.5 g of adsorbent was treated with 50 cm^3 of single or binary dyes mixture bearing solution with pre-determined initial dye concentrations (100-700 mg dm^{-3}). The flasks were shaken at 150 rpm for 2 days to ensure equilibrium was reached. The supernatant solution was separated from the adsorbent by filtration using syringe filter unit (Minisart) of 0.2 μm in size and then the equilibrium concentrations of dyes were measured by the spectrophotometer (Spekol 11, Carl Zeiss JENA).

Table 4. Comparison of isotherms parameters for the adsorption of BY 21 on FS and WS.

Model	Parameters	FS	WS
Langmuir	**R% (at equilibrium)**	92.82	67.63
	q_m (mg g^{-1})	76.92	71.43
	b (dm^3 g^{-1})	0.053	0.005
	R^2	0.946	0.781
Freundlich	**n**	1.54	1.33
	K_F (dm^3 g^{-1})	5.32	0.758
	R^2	0.929	0.946
Temkin	**A (dm^3 g^{-1})**	0.618	0.082
	B	5.92	12.04
	R^2	0.996	0.959

The single-component Langmuir and Freundlich isotherm models were applied to the adsorption equilibrium data for single-component and binary mixture. Equilibrium adsorption for binary system was also analyzed by using multi-component modified Langmuir and Sheindorf– Rebuhn–Sheintuch (SRS) models.

3.2.2.2. Multi-component models

3.2.2.2.1. Modified Langmuir model

Modified Langmuir model can be written for N-components in the mixture as follows:

$$q_{e,i} = \frac{q_{m,i} b_i C_i}{1 + \sum_{j=1}^{N} b_j C_j} \tag{12}$$

where: C_i and C_j are the concentrations of the adsorbates i and j remaining in liquid at equilibrium (mg dm^{-3}), $q_{e,i}$ is the equilibrium uptake of the adsorbate i in the multi-component system (mg g^{-1}). b_i and b_j are the Langmuir adsorption constants of the adsorbates (dm^3 g^{-1}) and $q_{m,i}$ is the Langmuir adsorption capacity of the adsorbate i (mg g^{-1}) that can be estimated from the fitting of the experimental data by the corresponding individual Langmuir isotherm equation.

3.2.2.2.2. Sheindorf–Rebuhn–Sheintuch (SRS) model

Sheindorf et al. derived a Freundlich-type multi-component adsorption isotherm, the Sheindorf–Rebuhn–Sheintuch (SRS) equation. The general SRS equation for a component *i* in an *N*-component system is given as:

$$q_i = K_i C_i \left(\sum a_{ij} C_j \right)^{n_i - 1} \tag{13}$$

where: q_i is the adsorption capacity of component *i* (mg g^{-1}); C_i and C_j are the concentrations of *i* and *j* in the equilibrium solution (mg dm^{-3}); K_i (dm^3 g^{-1}) and n_i are the Freundlich constants obtained for *i* in a single-component system; and a_{ij} is the competition coefficient for the adsorption of component *i* in the presence of component *j*.

3.2.2.3. Isotherm evaluation and fitting

The sum of the squares of the errors (*SSE*) function has been used to test the adequacy and accuracy of the fit of the four isotherm models with the experimental data:

$$SSE = \sum_{i=1}^{N} \left(q_{e,cal} - q_{e,exp} \right)_i^2 \tag{14}$$

where: the subscripts '*exp*' and '*cal*' indicate the experimental and calculated values, respectively and *N* is the number of measurements.

3.2.2.4. Equilibrium modeling for adsorption of Basic Blue 3 and Basic Red 18 on flax shives from single- and binary-component systems

Single-component Langmuir and Freundlich isotherm models applied on both single and binary systems with the aim to compare the maximum adsorption capacity from single solute solutions to that of binary solutions for each particular dye. The results for fitting of both models to adsorption data of single and binary systems are presented in Table 5.

Table 5 shows the maximum adsorption capacity (q_m) of FS for basic dyes from single and binary solutions. The same value for maximum adsorption capacity of FS was obtained for BB 3 and BR 18 dyes in single solution system as 66.67 mg g^{-1}, while in binary mixture it was increased to 71.34 mg g^{-1} and 76.92 mg g^{-1} for BB 3 and BR 18 dyes, respectively resulting in their synergistic effect.

The generally accepted explanation for this "cooperative" type of adsorption is that on adsorbent surfaces lateral attractive interactions between adsorbate molecules at the interface can cause enhanced adsorption of some adsorbates. Such proposed interactions are illustrated in the schematic representation of Fig. 7.

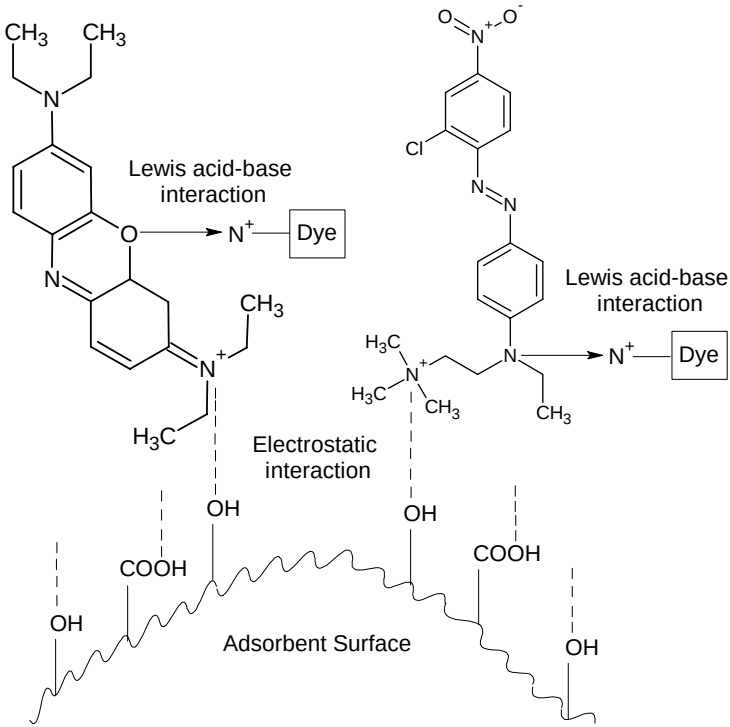

Fig. 7. Schematic representation for the proposed adsorbates-adsorbates and adsorbates-adsorbent interactions.

Table 5. Parameters of Langmuir and Freundlich isotherms for single (S) and binary (B) systems for FS.

System	Langmuir		Freundlich	
	q_m (mg g^{-1})	b (dm^3 g^{-1})	K_F (dm^3 g^{-1})	n
BB 3 (S)	66.67	0.254	17.14	0.355
BB 3 (B)	71.34	0.412	21.18	0.335
BR 18 (S)	66.67	0.106	11.09	0.415
BR 18 (B)	76.92	0.250	17.02	0.437

Table 6 summarizes the values of *SSE* for single-component and multi-component isotherms models. As elucidated by the table, the Freundlich and Langmuir models were the best suitable adsorption models for describing the adsorption of Basic Blue 3 in single and binary systems, respectively. For Basic Red 18, Langmuir model was the best one for fitting the adsorption equilibrium in single and binary systems.

Table 6. *SSE* values for single-component and multi-component isotherms models for FS.

System	Langmuir	Freundlich	Modified Langmuir	SRS model
BB 3 (S)	377.81	161.86		
BB 3 (B)	194.87	327.62	849.9	7.5E+12
BR 18 (S)	58.7	155.17		
BR 18 (B)	113.74	240.43	4168	3E+10

3.2.2.5. Equilibrium modeling for adsorption of Basic Blue 3 and Basic Red 18 on wheat straw from single- and binary-component systems

The possible reduction in dye adsorption capacity onto WS in binary mixtures was evaluated by comparing the maximum adsorption capacity from single dye solutions to that of binary dye solutions for each particular dye. The results of fitting of Langmuir and Freundlich models to adsorption data of single and binary systems are presented in Table 7.

Table 7 also shows the maximum adsorption capacity (q_m) of WS for basic dyes from single and binary solutions. The maximum adsorption capacities of WS for BB 3 and BR 18 dyes in single solution system were found as 90.91 mg g^{-1} and 142.86 mg g^{-1}, respectively, while in binary mixture it were decreased to 76.92 mg g^{-1} and 111.11 mg g^{-1}, respectively, resulting in their antagonistic behavior. This can be attributed in the main to the interaction between the dyes on the solid surface, with competition.

Table 7. Parameters of Langmuir and Freundlich isotherms for single (S) and binary (B) systems for WS.

System	Langmuir		Freundlich	
	q_m (mg g^{-1})	b (dm^3 g^{-1})	K_F (dm^3 g^{-1})	n
BB 3 (S)	90.91	0.054	7.89	0.579
BB 3 (B)	76.92	0.115	11.75	0.482
BR 18 (S)	142.86	0.010	2.01	0.816
BR 18 (B)	111.11	0.038	5.71	0.700

Table 8. *SSE* values for single-component and multi-component isotherms models for WS.

System	Langmuir	Freundlich	Modified Langmuir	SRS model
BB 3 (S)	296.07	219.35		
BB 3 (B)	187.47	97.23	642.11	6E+13
BR 18 (S)	184.12	450.02		
BR 18 (B)	76.67	169.54	4109.35	4.6E+11

The best fitting model is determined based on the lowest *SSE* values. Table 8 summarizes the values of *SSE* for single-component and multi-component isotherms models. Equilibrium data of BB 3 in single and binary systems fitted more adequately to the Freundlich adsorption isotherm. For BR 18, Langmuir model was the best one for fitting the adsorption equilibrium in single and binary systems.

3.2.2.6. Comparison between flax shives and wheat straw for adsorption of Basic Blue 3 and Basic Red 18 from single- and binary-component systems

In general, a mixture of different adsorbates may exhibit three possible types of behavior: synergism, antagonism and non-interaction. The maximum adsorption capacities of FS increased for both dyes in binary mixture as compared to single dye system due to synergistic effect between dyes. In case of WS, the binary solution exhibited inhibitory (antagonistic) adsorption for each dye, thereby resulting in a lower q_m).

Based on *SSE* values, the single-component Langmuir and Freundlich models were the best suitable adsorption models for describing the adsorption of basic dyes in single and binary systems on both FS and WS.

3.3. Adsorption kinetics

The study of adsorption kinetics in wastewater treatment is important since it provides valuable insights into reaction pathways and mechanism of adsorption process.

3.3.1. Adsorption kinetics for single-component systems
3.3.1.1. Description of experiment

The effects of important parameters such as initial dye concentration (100 – 400 mg dm^{-3}), adsorbent dose (4 – 20 g dm^{-3}), and stirring rate (60 – 160 rpm) on the kinetics of BY 21 adsorption onto FS and WS were studied at 20 ^{o}C. Experiments were carried out in a batch adsorber (a 2 dm^3 glass beaker) with a two-bladed impeller to stir the dye solution using Heidolph RZR 2100 motor. In all adsorption experiments, specific amount of adsorbent was mixed with 1.7 dm^3 dye solution. Samples (3-5 cm^3) for concentration measurements were withdrawn from the mixture at regular time intervals (from 1 min up to 660 min) using a syringe and immediately filtered using syringe filter unit (0.2 μm) to be ready for analysis.

3.3.1.2. Effect of operating parameters on kinetics of adsorption of Basic Yellow 21 on flax shives and wheat straw
3.3.1.2.1. Effect of initial dye concentration

The effect of initial concentration of BY 21 on the rate of adsorption onto FS and WS is illustrated in Figs. 8 and 9, respectively. The data indicated that, as expected, the dye

concentration decreases with time indicating that dye has been removed from the solution phase. Fig. 8 indicates that the adsorption of BY 21 on FS was very fast in the first 5 minutes, and thereafter the adsorption rate decreased gradually and then became constant at equilibrium time. The data for adsorption on WS (Fig. 9) also showed that the removal rate was rapid at initial stage with between 33.9 % and 50.9 % removal, depending on initial concentration, occurring within the first 30 minutes of the experiment. After that there is a gradual decrease in the rate of removal as the experiment proceeds until the equilibrium was reached.

The equilibrium time for adsorption on FS was found to be at 1–5 h based on the initial dye concentration, where equilibrium times increased by increasing initial dye concentration. It is also noted that equilibrium time for adsorption on WS was strongly dependent on initial concentration where the shortest equilibrium time (5 h) was observed at the lowest initial concentration of 100 mg dm^{-3} and the highest equilibrium time (10 h) was observed at the maximum initial concentration of 400 mg dm^{-3}. It is must be also noticed that the adsorption capacity, q_e of the adsorbents increased by increasing initial dye concentration. The adsorption capacity increased from 10.44 to 40.02 mg g^{-1} and from 7.24 to 24.32 mg g^{-1} as the initial BY 21 concentration increased from 100 to 400 mg dm^{-3} for FS and WS, respectively.

3.3.1.2.2. Effect of adsorbent dose

The effect of FS and WS dose, d on the removal rate of BY 21 was studied by varying the dosage from 4 to 20 g dm^{-3}. The experimental results are shown in Figs. 10 and 11 for FS and WS, respectively. It is observed that the rate of removal increased and the equilibrium time decreased from 5 h to 1 h and from 8 h to 3 h by increasing adsorbent dosage from 4 to 20 g dm^{-3} for FS and WS, respectively.

It is also found that increasing dose from 4 to 20 g dm^{-3}, increased the percentage of dye removal (R%) from 93.1 to 97.9% and from 59.3% to 69%, but decreased the adsorption capacity, q_e from 24.98 to 5.25 mg g^{-1} and from 23.24 to 3.83 mg g^{-1} for FS and WS, respectively. It is apparent that by increasing the dose of adsorbent, the number of sorption sites available for sorbent–solute interaction is increased, thereby resulting in the increased percentage dye removal from solution. On the other hand, the decrease in q_e with the increase in adsorbent dose may be due to overlapping of adsorption sites as a result of overcrowding of adsorbent particles.

3.3.1.2.3. Effect of stirring rate

The effect of the stirring rate on the kinetic process of BY 21 adsorption onto FS and WS was investigated by changing the impeller speed in the range of 60-160 rpm and the results are illustrated in Figs. 12 and 13 for FS and WS, respectively.

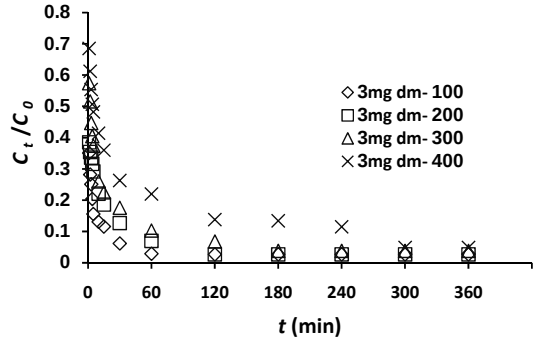

Fig. 8. Dimensionless concentration versus time of adsorption of BY 21 on FS at different initial dye concentrations.

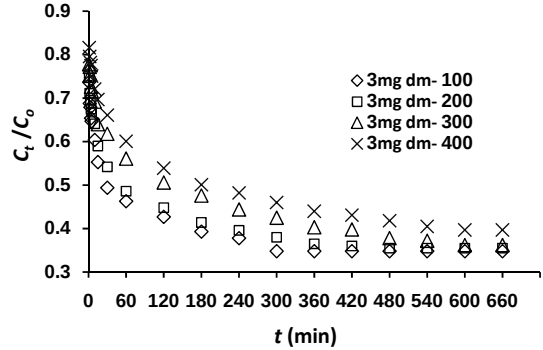

Fig. 9. Dimensionless concentration versus time of adsorption of BY 21 on WS at different initial dye concentrations.

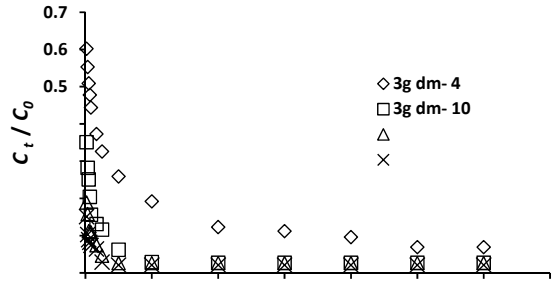

Fig. 10. Dimensionless concentration versus time of adsorption of BY 21 on FS at different adsorbent doses.

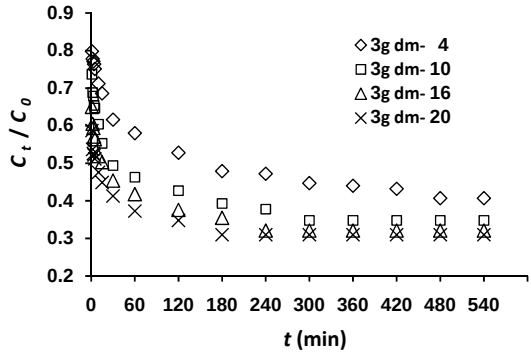

Fig. 11. Dimensionless concentration versus time of adsorption of BY 21 on WS at different adsorbent doses.

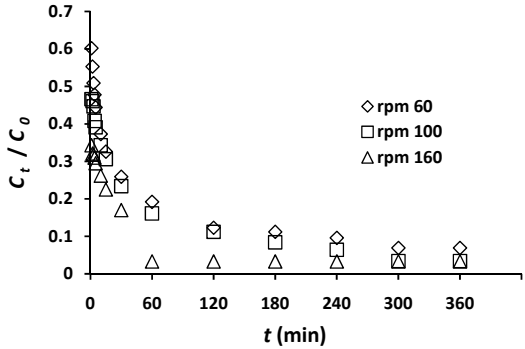

Fig. 12. Dimensionless concentration versus time of adsorption of BY 21 on FS at different stirring rates.

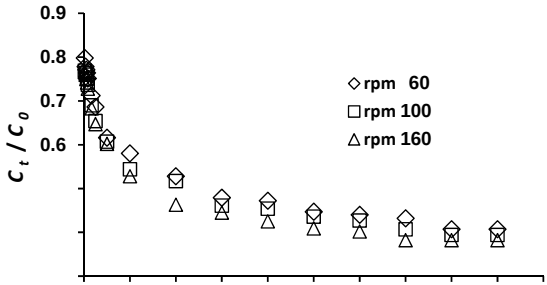

Fig. 13. Dimensionless concentration versus time of adsorption of BY 21 on WS at different stirring rates.

It is noted that the equilibrium time was dependent on stirring rate where the shortest equilibrium time for both FS and WS was obtained at the maximum stirring rate of 160 rpm. The rate of dye removal was not significantly influenced by the rate of stirring. This means that the mass transfer through the external film is not the rate controlling step and implies that intraparticle diffusion resistance needs to be included in the analysis of whole sorption process.

3.3.1.3. Kinetics modeling

3.3.1.3.1. The Pseudo-first order kinetic model

$$\ln(q_e - q_t) = \ln q_e - k_1 t \tag{15}$$

where: q_e and q_t are the values of amount adsorbed per unit mass at equilibrium and at any time t, respectively and k_1 is the pseudo-first order rate constant (min^{-1}). The values of k_1 and calculated equilibrium adsorption capacity, q_e, calc. can be obtained from the slope and intercept, respectively, of the linear plot of $\ln(q_e - q_t)$ versus t.

3.3.1.3.2. The Pseudo-second order kinetic model

The integrated linear form of the equation is written as:

$$\frac{t}{q_t} = \frac{1}{k_2 q_e^2} + \left(\frac{1}{q_e}\right) t \tag{16}$$

where: k_2 is the second order rate constant (g mg^{-1} min^{-1}).

The initial adsorption rate, h (mg g^{-1} min^{-1}) is expressed as:

$$h = k_2 . q_e^2 \tag{17}$$

Then Eq. (16) becomes,

$$\frac{t}{q_t} = \frac{1}{h} + \left(\frac{1}{q_e}\right) t \tag{18}$$

The plot of t/q_t versus t gives a linear relationship, which allows computation of k_2, h and calculated q_e.

3.3.1.3.3. Intraparticle diffusion model

In order to gain insight into the mechanisms and rate controlling steps affecting the kinetics of adsorption, the kinetic experimental results were fitted to the Weber's intraparticle diffusion model:

$$q_t = k_i t^{0.5} + I \tag{19}$$

where: I is the intercept and k_i is the intraparticle diffusion rate constant (mg g^{-1} $min^{0.5}$), which can be evaluated from the slope of the linear plot of q_t versus $t^{0.5}$.

3.3.1.4. Kinetics modeling for adsorption of Basic Yellow 21 on flax shives

The linear plots for both pseudo-first order ($\ln(q_e - q_t)$ versus t) and pseudo-second order (t/q_t versus t) models at different initial dye concentration are shown in Figs. 14 and 15, respectively. Similarly, linear plots were obtained for both models at different adsorbent doses and stirring rates. Table 9 lists the results of the rate constant studies for different initial dye concentrations, adsorbent doses and stirring rates by the pseudo-first order and pseudo-second order models together with intraparticle diffusion model. The best-fit model was selected based on the linear regression correlation coefficient, R^2 values.

The pseudo-second order model has the highest values of R^2 (> 0.997), and its calculated equilibrium adsorption capacities, are consistent with experimental data. These facts suggest that the adsorption kinetics fits very well the second-order kinetic model.

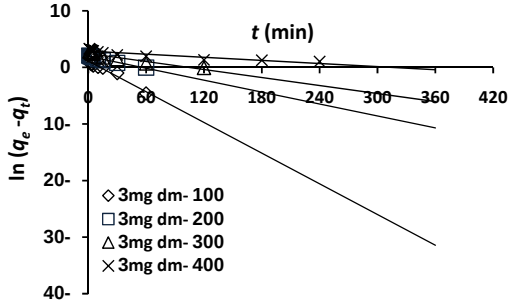

Fig. 14. Pseudo-first order kinetics for adsorption of BY 21 on FS at various initial dye concentrations.

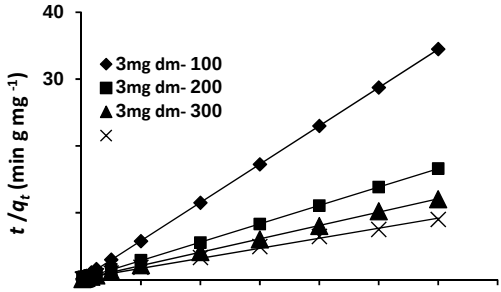

Fig. 15. Pseudo-second order kinetics for adsorption of BY 21 on FS at various initial dye concentrations.

Table 9. Rate constants for the pseudo-first order, pseudo-second order and intraparticle diffusion models for the adsorption of BY 21 on FS.

Factor	Pseudo-first order kinetic model				Pseudo-Second order kinetic model				Intraparticle diffusion model	
C_0 (mg dm^{-3})	q_e, exp. (mg g^{-1})	q_e, cal. (mg g^{-1})	K_1 (min^{-1})	R^2	q_e, cal. (mg g^{-1})	K_2 (g mg^{-1} min^{-1})	h, (mg g^{-1} min^{-1})	R^2	K_i (mg g^{-1} min$^{0.5}$)	R^2
100	10.44	3.04	0.090	0.970	10.53	0.113	12.53	1	0.256	0.977
200	21.66	7.13	0.035	0.969	22.22	0.023	11.35	0.999	0.72	0.981
300	29.33	11.55	0.023	0.907	30.3	0.011	10.1	0.999	0.773	0.946
400	40.02	17.9	0.009	0.860	40	0.004	6.4	0.997	0.636	0.92
d (g dm^{-3})										
4	24.98	10.05	0.012	0.925	25.64	0.0076	5	0.999	0.837	0.966
10	10.44	3.04	0.09	0.97	10.53	0.113	12.53	1	0.256	0.977
16	6.53	1.09	0.138	0.962	6.54	0.556	23.78	1	0.237	0.989
20	5.25	0.71	0.171	0.898	5.26	1.004	27.78	1	0.092	0.837
rpm										
60	24.98	10.05	0.012	0.925	25.64	0.0076	5	0.999	0.837	0.966
100	25.92	9.59	0.011	0.956	25.64	0.0084	5.52	0.999	1.118	0.988
160	25.95	8.22	0.027	0.989	25.64	0.0205	13.48	0.999	1.239	0.989

3.3.1.5. Kinetics modeling for adsorption of Basic Yellow 21 on wheat straw

The linear plots for both pseudo-first order ($\ln(q_e - q_t)$ versus t) and pseudo-second order (t/q_t versus t) models at different initial dye concentration are shown in Figs. 16 and 17, respectively. Similarly, linear plots were obtained for both models at different adsorbent doses and stirring rates. Table 10 lists the rate constants, k_1 and k_2, the calculated q_e, and the initial sorption rates, h, determined from the straight-line plots for pseudo-first order and pseudo-second order models at different conditions.

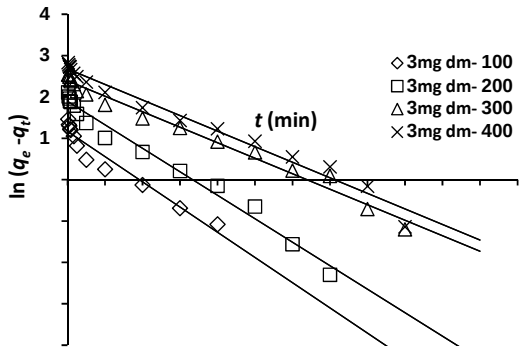

Fig. 16. Pseudo-first order kinetics for adsorption of BY 21 on WS at various initial dye concentrations.

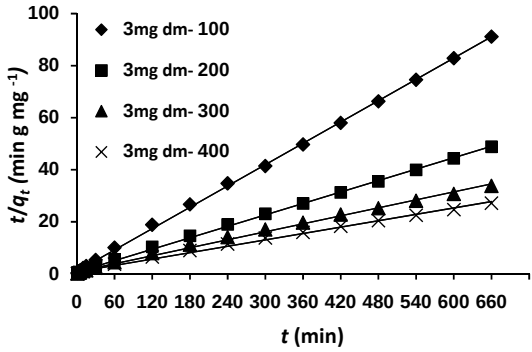

Fig. 17. Pseudo-second order kinetics for adsorption of BY 21 on WS at various initial dye concentrations.

It can be seen from Table 10 that there is an agreement between q_e, experimental and q_e, calculated values for the pseudo-second order model. Also, the correlation coefficients, R^2, of the pseudo-second order model are greater than 0.996 as compared to correlation coefficients for the pseudo-first order kinetics model that range from 0.917 to 0.983. Hence, the pseudo-second order model better represented the adsorption kinetics for BY 21 on WS.

Table 10. Rate constants for the pseudo-first order, pseudo-second order and intraparticle diffusion models for the adsorption of BY 21 on WS.

Factor	Pseudo-first order kinetic model				Pseudo-Second order kinetic model				Intraparticle diffusion model	
C_0 (mg dm^{-3})	q_e, exp. (mg g^{-1})	q_e, cal. (mg g^{-1})	K_1 (min^{-1})	R^2	q_e, cal. (mg g^{-1})	K_2 (g mg^{-1} min^{-1})	h, (mg g^{-1} min^{-1})	R^2	K_i (mg g^{-1} min$^{0.5}$)	R^2
100	7.24	3.21	0.010	0.938	7.35	0.019	1.03	0.999	0.130	0.993
200	13.52	6.64	0.009	0.983	13.7	0.008	1.5	0.999	0.226	0.991
300	19.52	10.95	0.006	0.983	19.61	0.003	1.15	0.996	0.424	0.994
400	24.32	14.54	0.006	0.978	24.39	0.002	1.19	0.996	0.562	0.982
d (g dm^{-3})										
4	16.45	8.87	0.006	0.969	16.67	0.004	1.11	0.997	0.476	0.997
10	7.24	3.21	0.010	0.938	7.35	0.019	1.03	0.999	0.130	0.993
16	4.71	1.73	0.012	0.940	4.76	0.043	0.97	0.999	0.086	0.984
20	3.83	1.17	0.016	0.917	3.86	0.087	1.3	0.999	0.076	0.973
rpm										
60	16.45	8.87	0.006	0.969	16.67	0.0040	1.11	0.997	0.476	0.997
100	16.82	8.91	0.007	0.969	16.95	0.0047	1.35	0.997	0.329	0.951
160	17.15	8.98	0.008	0.969	17.54	0.0051	1.57	0.998	0.220	0.989

3.3.1.6. Comparison between flax shives and wheat straw for adsorption kinetics parameters of Basic Yellow 21

The results of kinetic studies for the adsorption of BY 21 on both FS and WS implied that the equilibrium time is strongly dependent on initial dye concentration, adsorbent dose and stirring rate. However, adsorption of BY 21 dye by FS occurred at a faster rate in comparison to WS. The time taken to reach equilibrium was shorter in the case of FS, compared to WS which showed longer equilibrium times at all the different conditions.

3.3.1.7. Mechanism of adsorption of Basic Yellow 21 on flax shives and wheat straw

Prediction of the rate-limiting step is an important factor to be considered in sorption process. Sorptive removal of dyes from aqueous solution involves solute transfer, which is usually characterized by either external mass transfer (boundary layer diffusion) or intraparticle diffusion or both. The overall rate of sorption will be controlled by the slowest step, which would be either film diffusion or pore diffusion.

However, the controlling step might be distributed between intraparticle and external transport mechanism. Whatever may be the case external diffusion will be involved in the sorption process.

The sorption of BY 21 onto FS and WS particles may be controlled due to film diffusion at earlier stages and as the adsorbent particles gets loaded with dye ions, the sorption process may be controlled due to intraparticle diffusion. The possibility of intraparticle diffusion resistance affecting adsorption was explored by using the intraparticle diffusion model.

Figs. 18 and 19 show the plots between q_t versus $t^{0.5}$ for BY 21 onto FS and WS particles, respectively, at different initial dye concentrations. Similar plots were obtained at different adsorbent doses and stirring rates for both FS and WS. From the figures, the sorption process tends to be followed by two phases. It was found that an initial linear portion ended with a smooth curve followed by second linear portion. The two phases in the intraparticle diffusion plot suggests that the sorption process proceeds by surface sorption and the intraparticle diffusion. The initial curved portion of the plot indicates boundary layer effect while the second linear portion is due to intraparticle or pore diffusion.

The intercept, I of the plot (q_t versus $t^{0.5}$) reflects the boundary layer effect. Larger the I, greater is the contribution of the surface sorption in the rate-limiting step.

If the plot of q_t versus $t^{0.5}$ is linear and passes through the origin, then intraparticle diffusion is the sole rate-limiting step. However, the linear plots at all different conditions did not pass through the origin (Figures are not shown).

This indicates that the intraparticle diffusion was not the only rate controlling step. This also confirms that the adsorption of BY 21 on FS and WS was a multi-step process, involving adsorption on the external surface and diffusion into the interior.

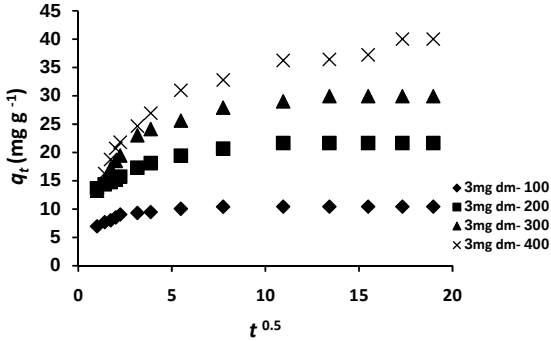

Fig. 18. Intraparticle diffusion plots for BY 21 adsorption on FS at various initial dye concentrations.

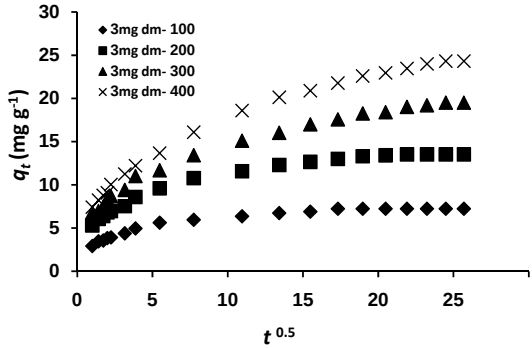

Fig. 19. Intraparticle diffusion plots for BY 21 adsorption by WS at various initial dye concentrations.

3.3.2. Adsorption kinetics for single- and binary-component systems

Kinetics of adsorption of BB 3 and BR 18 from aqueous solution onto FS and WS were evaluated in single and binary systems.

3.3.2.1. Kinetics experiment

The kinetics of BB 3 and BR 18 adsorption in single and binary adsorption systems onto FS and WS were studied at 20 ^{o}C. Experiments were carried out in a standard agitated reactor experimental set-up (a 2 dm^3 glass beaker) with a two-bladed impeller to stir the dye solution

using Heidolph RZR 2100 motor. In all adsorption experiments, a pre-selected amount of adsorbent (17 g) was dispersed in 1.7 dm^3 of dye solution of 400 mg dm^{-3} (in single and binary systems) while being constantly stirred by a mechanical stirrer at a speed of 60 rpm. Samples (3-5 cm^3) were withdrawn from the mixture at regular time intervals (from 1 min up to 540 min) using a syringe and immediately filtered using syringe filter unit (0.2 μm) and analyzed by means of the spectrophotometer.

3.3.2.2. Kinetics modeling for adsorption of Basic Blue 3 and Basic Red 18 on flax shives from single - and binary-component systems

Figs. 20 and 21 show the variation of BB 3 and BR 18 uptakes, respectively in single and binary systems with time. As seen from figures, the adsorption was rapid in the initial stage since there were many available sites for adsorption on the adsorbent and a high concentration of dye molecules in solution. Then the adsorption rate slow down toward the end due to fewer sites was available and the concentration of dye in solution decreased.

Figs. 20 and 21 also show the comparison of single and binary systems for BB 3 and BR 18 adsorption on FS. It is seen that BB 3 and BR 18 adsorption is increased in binary system, which suggests a synergetic adsorption.

The pseudo-first order and pseudo-second order models were used to describe the kinetic data for the adsorption of BB 3 and BR 18 on FS from single and binary systems. The linear plots for both pseudo-first order and pseudo-second order models are shown in Figs. 22 and 23, respectively. The kinetic parameters obtained are collected in Table 11.

Table 11 indicates that the pseudo-second order model has the highest values of R^2 and its calculated equilibrium adsorption capacities are consistent with experimental capacities. These facts suggest that the adsorption kinetics for BB 3 and BR 18 on FS in single and binary systems fits very well the second-order kinetic model.

Table 11. Kinetic parameters for the adsorption of BB 3 and BR 18 on FS in single and binary systems.

Dyes	Adsorption system	q_e, exp. (mg g^{-1})	Pseudo-first order			Pseudo-second order		
			q_e, cal. (mg g^{-1})	K_1 (min^{-1})	R^2	q_e, cal. (mg g^{-1})	K_2 (g mg^{-1} min^{-1})	R^2
BB 3	BB 3-S	39.31	7.99	0.014	0.869	40	0.010	1
	BB 3-B	42.13	6.43	0.008	0.970	43.38	0.007	0.999
BR 18	BR 18-S	39.28	4.87	0.030	0.916	40	0.040	1
	BR 18-B	43.46	4.08	0.010	0.967	43.38	0.020	1

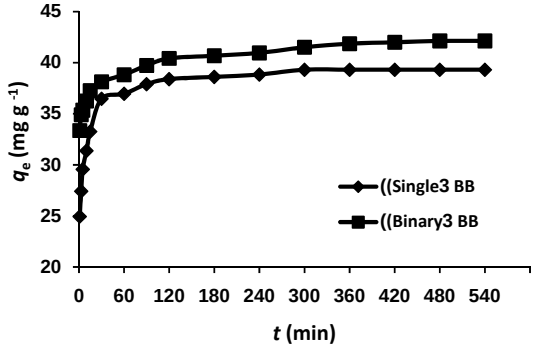

Fig. 20. Effect of contact time on the amounts of BB 3 adsorbed on FS in single and binary systems.

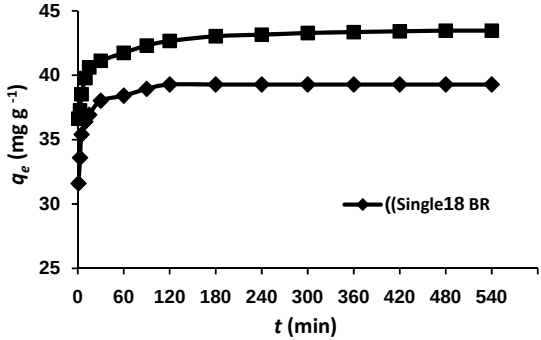

Fig. 21. Effect of contact time on the amounts of BR 18 adsorbed on FS in single and binary systems.

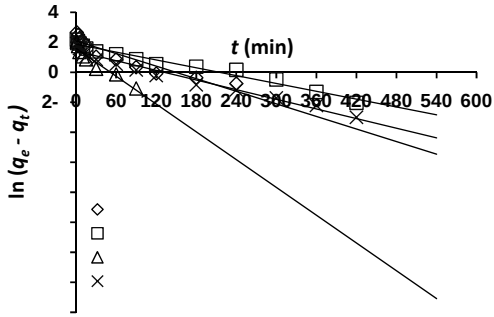

Fig. 22. Pseudo-first order kinetics for adsorption of BB 3 and BR 18 on FS in single and binary systems.

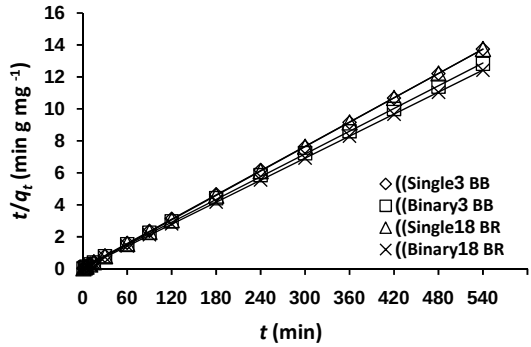

Fig. 23. Pseudo-second order kinetics for adsorption of BB 3 and BR 18 on FS in single and binary systems.

3.3.2.3. Kinetics modeling for adsorption of Basic Blue 3 and Basic Red 18 on wheat straw from single- and binary-component systems

Figs. 24 and 25 show the effect of the contact time on the amounts of dyes adsorbed in single and binary dye systems for BB 3 and BR 18, respectively. As contact time increases, dye uptake increase initially, and then become almost stable, denoting attainment of equilibrium. As can be also seen from the figures, the adsorption capacities decreased for both dyes after adsorption in binary systems, indicating the antagonistic behavior.

Plots of pseudo-first order and pseudo-second order models have been demonstrated in Figs. 26 and 27, respectively. Modeling of kinetics models and parameters obtained from the pseudo-first- and the second-order models are given in Table 12. It can be seen that the correlation coefficients, R^2, of the pseudo-second order model are close to 1 as compared to correlation coefficients for the pseudo-first order kinetics model that range from 0.881 to 0.961.

Table 12. Kinetic parameters for the adsorption of BB 3 and BR 18 on WS in single and binary systems.

Dyes	Adsorption system	q_e, exp. (mg g^{-1})	Pseudo-first order			Pseudo-second order		
			q_e, cal. (mg g^{-1})	K_1 (min^{-1})	R^2	q_e, cal. (mg g^{-1})	K_2 (g mg^{-1} min^{-1})	R^2
BB 3	BB 3-S	39.33	7.34	0.012	0.961	40	0.009	0.999
	BB 3-B	38.07	12.9	0.010	0.961	38.46	0.004	0.999
BR 18	BR 18-S	40.66	6.64	0.016	0.881	41.67	0.014	1
	BR 18-B	39.02	8.46	0.008	0.925	40	0.005	0.999

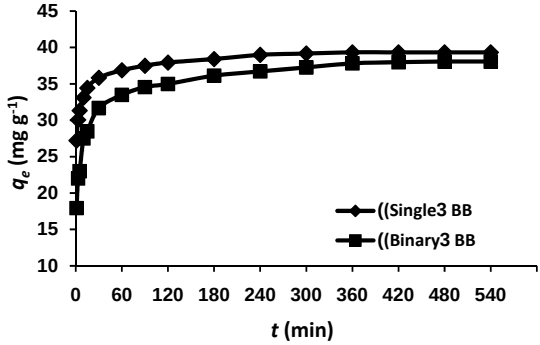

Fig. 24. Effect of contact time on the amounts of BB 3 adsorbed on WS in single and binary systems.

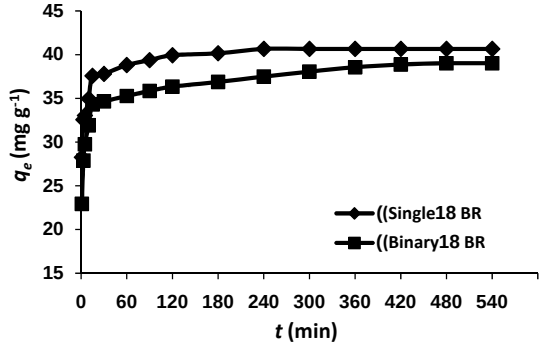

Fig. 25. Effect of contact time on the amounts of BR 18 adsorbed on WS in single and binary systems.

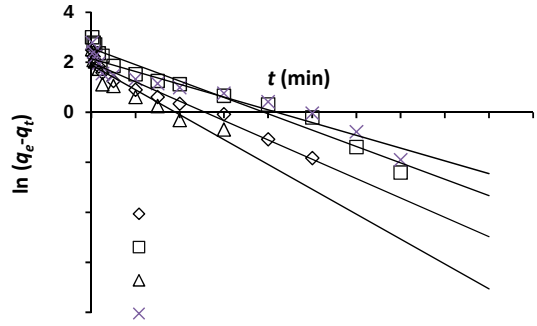

Fig. 26. Pseudo-first order kinetics for adsorption of BB 3 and BR 18 on WS in single and binary systems.

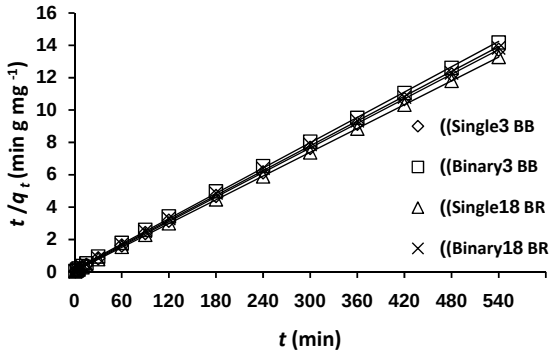

Fig. 27. Pseudo-second order kinetics for adsorption of BB 3 and BR 18 on WS in single and binary systems.

Adsorption capacities calculated (q_e, cal.) by the pseudo-second order were also close to those obtained from experiments (q_e, exp.). Hence, the pseudo-second-order model provides the best correlation for the adsorption process of BB 3 and BR 18 on WS in single- and binary-component systems.

3.3.2.4. Comparison between flax shives and wheat straw for kinetics modeling for adsorption of Basic Blue 3 and Basic Red 18 from single- and binary-component systems

The equilibrium time was shorter in the case of FS, compared to WS which showed longer equilibrium times for the adsorption of BB 3 and BR 18 from single-component systems. This may be due to the fact that FS has a lower particle size as compared to WS that has a larger particle size.

For both FS and WS, the kinetic measurements indicated that the adsorption process (From single- and binary-component systems) follows pseudo-second order kinetics. The adsorption capacities of FS increased for both dyes in binary mixture as compared to single dye system due to synergistic effect between dyes. In case of WS, the binary solution exhibited antagonistic adsorption for each dye, thereby resulting in a lower q_e.

Conclusions

1. The present study shows the effectiveness of the agricultural wastes, flax shives (FS) and wheat straw (WS) as low-cost adsorbents for the removal of Basic Yellow 21 (BY 21) from single solution and for single and binary removal of Basic Blue 3 (BB 3) and Basic Red 18 (BR 18) dyes from aqueous solutions.

2. Equilibrium data obtained for the adsorption of Basic Yellow 21 on both flax shives and wheat straw were modeled using three isotherm models: Langmuir, Freundlich and Temkin. The best-fit equilibrium model was determined based on the linear regression correlation coefficient R^2. The comparison of R^2 values indicated that equilibrium isotherms were well described by the Temkin model better than that of Langmuir and Freundlich.

3. The single-component Langmuir and Freundlich isotherm models were applied to the adsorption equilibrium data of both flax shives and wheat straw for Basic Blue 3 and Basic Red 18 in single-component and binary mixture systems. Equilibrium adsorption for binary system was also analyzed by using multi-component modified Langmuir and Sheindorf–Rebuhn–Sheintuch (SRS) models. The best fitting model is determined based on the lowest sum of the squares of the errors (*SSE*) values. Based on *SSE* values, the single-component Langmuir and Freundlich models were the best suitable adsorption models for describing the adsorption of Basic Blue 3 and Basic Red 18 in single and binary systems on both flax shives and wheat straw.

4. The maximum adsorption capacities for Basic Yellow 21, Basic Blue 3 and Basic Red 18 from single systems were 76.92, 66.7, 66.7 mg g^{-1} and 71.43, 90.91, 142.86 mg g^{-1} for flax shives and wheat straw, respectively.

5. The maximum adsorption capacities of flax shives increased for both Basic Blue 3 and Basic Red 18 in binary mixture to be 71.34 and 76.92 mg g^{-1}, respectively, as compared to single dye system due to synergistic effect between dyes. In case of wheat straw, the binary solution exhibited competitive adsorption for each dye, thereby resulting in a lower adsorption capacity, where the maximum adsorption capacities of wheat straw decreased for both Basic Blue 3 and Basic Red 18 in binary mixture to be 76.92 and 111.11 mg g^{-1}, respectively.

6. The effect of operating parameters such as initial dye concentration (100 – 400 mg dm^{-3}), adsorbent dose (4 – 20 g dm^{-3}) and stirring rate (60 – 160 rpm) on the kinetics of Basic Yellow 21 adsorption onto flax shives and wheat straw was investigated at 20 ^{o}C. The results implied that the equilibrium time is strongly dependent on initial dye concentration, adsorbent dose and stirring rate, where the equilibrium time was found to

increase with the increase in initial dye concentration, and found to decrease with the increase in adsorbent dose and stirring rate.

7. The adsorption of Basic Yellow 21, Basic Blue 3 and Basic Red 18 by flax shives from single and binary solutions occurred at a faster rate in comparison to wheat straw. The time taken to reach equilibrium was shorter in the case of flax shives, compared to wheat straw. For both adsorbents, the kinetic measurements indicated that the adsorption process for dyes follows pseudo-second order kinetics, suggesting chemisorption mechanism.

8. The studying of intraparticle diffusion model for the adsorption of Basic Yellow 21onto flax shives and wheat straw indicated that the dye uptake process was found to be controlled by external mass transfer at earlier stages and by intraparticle diffusion at later stages. So, the adsorption mechanism was suggested to be complex, consisting of both surface adsorption and pore diffusion. It must be also noted by the chemical characterization of adsorbents that both flax shives and wheat straw are composed mainly of cellulose, hemicellulose and lignin, which provides binding sites (anionic) for the basic (cationic) dyes due to the presence of functional groups such as hydroxyl, carboxyl, methoxy, phenols, etc.

Recommendations

There are large quantities of flax shives and wheat straw produced in Egypt that create disposal problem resulting in environmental pollution. So, the use of these agricultural wastes as low-cost adsorbents for removing dyes from wastewater presents many attractive features especially their contribution in the reduction of costs for waste disposal, therefore contributing to environmental protection. Furthermore, the regeneration of the spent flax shives and wheat straw adsorbents is not recommended because of it is waste materials that is available at almost no cost and it can be burnt with the sorbed dye as a source of energy.

There is scarce data available for the competitive adsorption of dyes. Therefore, more research should be conducted in this direction for adsorption of dyes in presence of other contaminants such as phenols, metals, etc. It is further suggested that the research should not limit to only lab scale batch studies, but pilot-plant studies should also be conducted utilizing agricultural wastes adsorbents to check their feasibility on commercial scale.

List of publications from PhD thesis

1. T.F. Hassanein, B. Koumanova, Decolourisation of waters using flax shives wasted from agriculture, *Fresenius Environ. Bull.*, 19 (9) 1894-1905 (2010).

2. T.F. Hassanein, B. Koumanova, Evaluation of adsorption potential of the agricultural waste wheat straw for basic yellow 21, *J. Univ. Chem. Technol. Met.(Sofia)*, 45 (4) 407-414 (2010).

3. T.F. Hassanein, B. Koumanova, Binary mixture sorption of basic dyes onto wheat straw, *Bulg. Chem. Commun.*, Article in press, (2011).

- ***Scientific Conferences*:**

1. T.F. Hassanein, B. Koumanova, DECOLOURISATION OF WASTEWATER BY AGRICULTURAL WASTE "*FLAX SHIVES* ", **6th Scientific Poster Session for Young Scientists**, 21 May 2009, UCTM, Sofia, Bulgaria.

2. T.F. Hassanein, B. Koumanova, DECOLOURISATION OF WATERS USING *FLAX SHIVES* WASTED FROM AGRICULTURE, **the 15th International Symposium on Environmental Pollution and its Impact on Life in the Mediterranean Region,** 7 – 11 October 2009, Bari, Italy.

3. T.F. Hassanein, B. Koumanova, EQUILIBRIUM MODELING OF SINGLE AND BINARY ADSORPTION OF BASIC DYES ONTO FLAX SHIVES, **7th Scientific Poster Session for Young Scientists**, 19 May 2010, UCTM, Sofia, Bulgaria.

4. T.F. Hassanein, B. Koumanova, SYNERGISTIC EFFECT FOR BI-COMPONENT ADSORPTION OF BASIC DYES ONTO *FLAX SHIVES* WASTED FROM AGRICULTURE, **19th International Congress of Chemical and Process Engineering CHISA 2010 and the 7th European Congress of Chemical Engineering ECCE-7,** 28 August - 1 September 2010, Prague, Czech Republic .

- ***Other Publications*:**

M.K. Zahran, T.F. Hassaneen, Utilization of the Egyptian flax shives for the removal of cadmium ions from aqueous solutions, *Egyp. J. Chem.*, 50 (2) 247-257 (2007).